Available online at www.eccomasproceedia.org
Eccomas Proceedia COMPDYN (2025) 1-10

ECCOMAS
Proceedia

COMPDYN 2025
10th ECCOMAS Thematic Conference on
Computational Methods in Structural Dynamics and Earthquake Engineering
M. Papadrakakis, M. Fragiadakis (eds.)
Rhodes Island, Greece, 15-18 June 2025

FEASIBILITY OF SEMI-ACTIVE MOVABLE SHEAR KEY FOR SEISMIC VIBRATION CONTROL OF BRIDGES

B. Neethu[1], I. Mikes[1], A. Giaralis[1], A. Kappos [1]

[1] Department of Civil and Environmental Engineering, Khalifa University, Abu Dhabi, UAE

Abstract

Movable shear keys (MSKs) have been proposed as a novel approach to optimizing the dynamic performance of bridges. Unlike traditional shear keys whose position is fixed, the MSKs can adjust their position in response to an ongoing ground motion, enhancing the overall seismic performance of the bridge. Thus far, MSKs have been developed as 'passive' devices, adjusting their position in a one-off operation based on the intensity of the oncoming earthquake estimated using a sensor in the area.

The semi-active MSK proposed herein is designed to engage or disengage based on real-time displacement-based thresholds, allowing it to act only when seismic response approaches the thresholds. This adaptability is achieved using a closed-loop feedback control strategy, which dynamically shifts, locks or unlocks the shear keys in real-time, to maximise the safety of the critical components of the bridge.

The effectiveness and robustness of the proposed semi-active control strategy are evaluated by simulating the response of a bridge with MSKs using nonlinear response history analysis. The numerical results indicate that the proposed control system is effective in reducing the peak responses of the bridge components. Additionally, a sensitivity analysis reveals that the performance of the controller is influenced by the selection of, a safety factor limit that determines when the semi-active device is activated. Through this analysis, an optimum value of this factor is identified, which maximizes the performance of the control system. Furthermore, the results indicate that the controller remains effective even under varying initial gap sizes, highlighting its robustness and adaptability.

Keywords: bridge joints; optimum seismic performance; dynamic intelligent bridge; shear keys; active control; response history analysis; OpenSees.

ISSN:2623-3347
Peer-review under responsibility of the organizing committee of COMPDYN 2025.
doi: 10.7712/120125.12387.25298

1 INTRODUCTION

Bridges are critical components of transportation infrastructure, serving as essential lifelines during emergencies caused by natural or man-made hazards. Although the seismic response of bridges conforming to modern code provisions is generally very satisfactory, examples of catastrophic bridge failure are found all over the world during moderate to strong earthquakes [1]. Past earthquakes such as the 2008 Sichuan, 2010 Chile, and 2011 Tohoku earthquakes, have caused structural damage and collapse, often resulting in significant disruptions to mobility and delays in emergency response [2]. Structural vibration control has emerged as an effective technology for earthquake mitigation. Over the years, extensive research has been conducted to formulate successful approaches for controlling seismic vibrations and alleviating the adverse consequences of earthquakes on structures. Researchers have studied different passive, active, semi-active, and hybrid control methods [3] for seismic response control of structures. While numerous passive technologies have been successfully deployed in civil engineering structures, to mitigate vibrations, the application of active, semi-active and hybrid control in full-scale bridges has been relatively limited [4]. This reluctance is often due to high capital and maintenance costs that are deemed to outweigh potential benefits from limiting damage by control systems. Nevertheless, the severe consequences of earthquake damage to bridges underscore the need for reliable, low-cost control systems. Despite advancements in earthquake-resistant bridge design, some aspects of seismic behaviour remain underexplored, for instance the impact of bridge joints. Modern seismic codes, such as Eurocode 8 [5] and Caltrans guidelines [6], overlook this aspect, which may be addressed either in an empirical way or through innovative solutions.

In this context, a novel concept of a dynamic intelligent (DI) bridge to optimize its dynamic performance was introduced by Kappos [7]. The concept stems from the observation that varying boundary conditions can lead to a more favourable dynamic response of a bridge, depending on the intensity and frequency content of the dynamic input. Unlike traditional shear keys, which are fixed and unable to adapt to varying seismic demands, movable shear keys (MSKs) offer the unique capability to dynamically alter boundary conditions, by adjusting their position in response to earthquake vibrations.

Initially, MSKs were developed as adaptive passive devices [8], designed to adjust the joint gap to a specific size, predetermined based on the seismic intensity. The semi-active MSK proposed in this study builds upon this concept by introducing real-time adaptability. The proposed MSK is a stopper, positioned on the abutment seat using a threaded bar mechanism that can be activated to move towards or away from the deck with minimal power input. This adaptability is achieved using a closed-loop feedback control strategy, which dynamically shifts, locks or unlocks the shear keys in real time, to maximise the safety of the critical components of the bridge. The semi-active control system is first described, and its effectiveness is evaluated by simulating the response of a bridge with MSKs using nonlinear response history analysis.

2 SEMI-ACTIVE CONTROL METHODOLOGY

The primary objective of the proposed semi-active control system is to achieve effective seismic vibration control with low power consumption and computational effort. Unlike traditional active control systems, the MSK does not generate forces opposing the vibration of a structure; instead, it modifies bridge boundary conditions by transitioning between open and closed states. This study implements a threshold-based binary control strategy, enabling the MSK to switch between on-off positions efficiently. In the context of semi-active MSKs, this means that the shear key either fully engages with the bridge deck or remains completely disengaged, depending on real-time displacement measurements and seismic demand.

The proposed control algorithm is developed to choose the optimum status (close or open) of the MSK in either direction of a bridge. The gap size is controlled in the longitudinal direction between the backwall and the deck and in the transverse between the deck and the shear keys. The control decision relies on a threshold-based switching mechanism, wherein the system continuously registers all the key displacement responses associated with different failure modes and switches between states when a limiting threshold displacement value is exceeded.

The control methodology starts with the definition of displacement thresholds. These thresholds are selected according to the safety-factor-based methodology developed by Mikes and Kappos [8]. The safety factor represents the margin of safety by using the capacity-to-demand ratio to assess the likelihood of exceeding specific threshold values associated with various limit states (LS). Two limit states are considered in the present study which are LS2-Operationality (bridge remains open to traffic) and LS4-Collapse prevention/Life safety. The limit state threshold values are selected based on the earlier study by Mikes et al.[9]. The bridge model is set up in *OpenSees* and is subjected to a set of nonlinear response history analyses (NLRHA). Based on the responses of the bridge subjected to NLRHA the engineering demand parameters (E_j) for the j critical components of the bridge (piers, bearings, abutments, shear keys) are calculated for each considered limit state i $\{i=LS2, LS4\}$.

As the proposed control methodology is displacement-driven, the engineering demand parameters (E_j) considered for the study are pier drifts, bearing deformations (which are proportional to the displacement at their location), displacement of the top of the backwall and displacement of the shear keys (normal keys or MSKs). The component safety factor $\lambda_{i,j}(A_g)$ corresponding to (E_j) is calculated based on the limit state thresholds ($d_{i,j}$) for each limit state as:

$$\lambda_{i,j}(A_g) = \frac{d_{i,j}}{E_j(A_g)}. \tag{1}$$

For each LS considered and each intensity of the earthquake, herein quantified by the peak ground acceleration (PGA), A_g,the global safety factor $\lambda_i(A_g)$ is calculated as the lowest component safety factor $\lambda_{i,j}$ among the considered bridge components in a certain direction, i.e.

$$\lambda_i(A_g) = min\ \lambda_{i,j} \tag{2}$$

The proposed semi-active control strategy aims to maximize the global safety factor of the bridge for the specified limit state and seismic intensity. With this as the primary objective, the global safety factor λ_i, calculated at each time step of the NLRHA using Equation 2, serves as the input to the feedback control loop. The controller dynamically adjusts the end joint gaps to increase λ_i, thereby improving the protection of the most critical bridge component.

The feedback control loop starts by taking the input to the controller which is the global safety factor at each time step. At each time-step, the controller compares the global safety factor λ_i with a predefined limiting value of the global safety factor ($\lambda_{lim,i}$) for the limit state (i) that is currently considered.

The selection of the values of $\lambda_{lim,i}$ plays a crucial role in the performance of the controller as these values govern the activation of the MSKs. The activation of the controller is enabled when the value of any of the measured structural responses of the component comes close to the exceedance of the limit states. To maintain a safety margin, a value greater than 1 is chosen for $\lambda_{lim,i}$. The controller first checks for the exceedance of LS2 and the value of the $\lambda_{lim,LS2}$. If LS2 is exceeded, the controller adjusts the gap based on the LS4 thresholds. A parametric study to choose the best value of the limiting global safety factors ($\lambda_{lim,LS2}$, $\lambda_{lim,LS4}$) for each limit state is conducted in the case study presented in Section 4.

Upon activation, the controller evaluates the component safety factor ($\lambda_{i,j}$) values at each time step to identify the most critical component. The decision for the gap updating is made based on the identified most critical component which can have the following scenarios:

a. If the critical component *j=piers or j=bearings*, the gap must be closed to enable the load transfer from these components to the abutment-backfill system.
b. If the critical component *j=abutment*, the gap must be opened to relieve it from all the forces caused by gap closure which could be achieved by a mechanism to disengage the abutment from the deck.

3 CASE STUDY

3.1 Modelling of the bridge and seismic action

To evaluate the performance of the proposed semi-active MSK system, a 99-meter-long reference bridge with ductile piers is selected as a case study. This bridge is a more cost-effective design of an actual three-span overpass on the Egnatia Motorway in Northern Greece which was used in the study of the adaptive passive MSK proposed by Mikes and Kappos [8]. The bridge has a 45 m central span, two 27 m outer spans, and a 10 m-wide prestressed concrete box girder monolithically connected to two cylindrical piers (1.2 m diameter, heights of 5.9 m and 7.9 m). The deck is supported by seat-type abutments (5.6 m and 5.7 m high) with 2.45 m backwalls and elastomeric bearings (350 × 450 × 181 mm, 77 mm rubber thickness). The bridge, resting on relatively firm cohesive soil corresponding to Class C (Eurocode 8)[5], is supported by 6 m × 6 m × 1.5 m footings. The finite element 'spine' model of the bridge (see Figure 1) is developed in *OpenSees* and consists of 3D beam-column elements and non-linear spring elements to capture the material non-linearities and the joint gaps. Pier nonlinearity is represented by plastic hinges at both ends, while soil-pier-foundation interaction is modelled using equivalent linear soil springs, with stiffness calculated using standard procedures [10]. The elastomeric bearings at the end of the deck were modelled as bilinear springs under horizontal shear and as elastic springs under flexure and axial load, as recommended in [11].

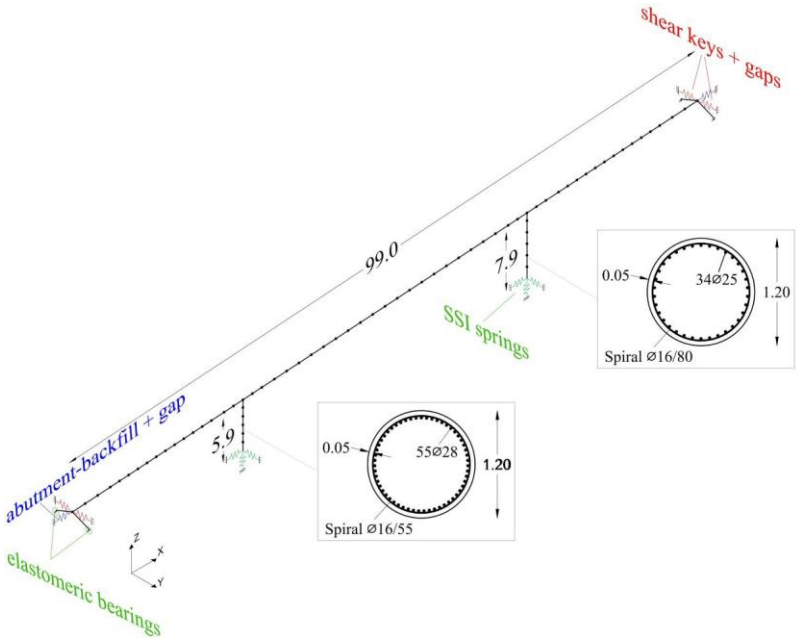

Figure 1 Structural model of the case-study bridge

The present study focuses on evaluating the performance of the proposed control system in the longitudinal direction of the bridge. The abutment-backfill system is modelled by incorporating a hinging mechanism in the backwall. The longitudinal passive resistance of the abutment-backfill system, up to its peak strength, is estimated based on the model developed at UCLA [12], based on a combination of test results and numerical studies. The hinging backwall mechanism is different from the 'shearing-off' backwall encouraged by Western US seismic design [6], where detachment occurs upon deck impact, and is clearly the most common solution in Europe and most other areas. To accurately capture the behaviour of the abutment-backfill system, the constitutive model of the system was modelled using the 'Hyperbolic Gap Softening material' developed by Mikes & Kappos [13] as a new class within the 'Uniaxial Material' in *OpenSees*. This model is an improved and extended version of the Hyperbolic Gap material which allows the user to define a post-peak descending linear segment followed by a residual force segment to accurately represent the complete response of the abutment-backfill system, as observed in relevant experimental tests (e.g. [14]).

To model the abutment-backfill system, this study adopts a simplified approach, consistent with the methodology outlined in the previous study by Mikes and Kappos [15]. This approach represents the entire abutment-backfill system using nonlinear springs positioned at each end of the deck. The backbone curve for these springs is derived from a pushover analysis of the abutment-backfill system, modelled in detail, incorporating the entire abutment using 3D beam-column elements. Plastic hinge formation was considered at the base of both the backwall and the stem wall. The backfill was represented by a series of springs, using the UCLA model. This detailed model was used to generate the pushover curve, which was then calibrated to the hyperbolic constitutive law of the Hyperbolic Gap Softening Material proposed in [13]. The curve fitting (Figure 2) was carried out, via optimisation using sum of squared errors (SSE) as the objective function.

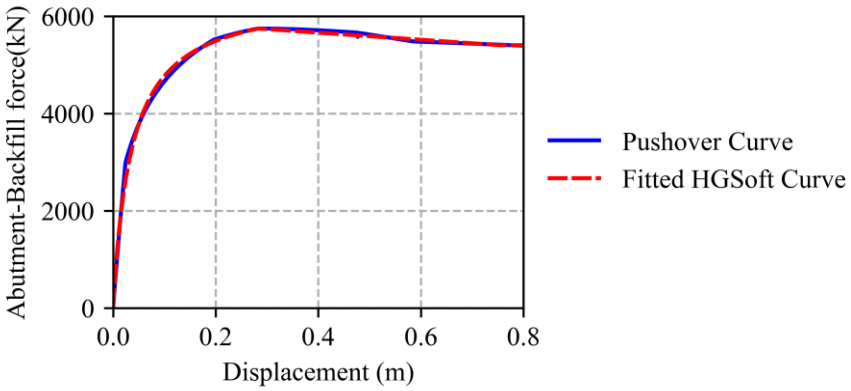

Figure 2 Fitted resistance curve of the abutment-backfill system

Based on the geometric details and the material properties of the bridge, two finite element models of the bridge in the longitudinal direction were developed in *OpenSees*. The first model of the bridge included the proposed semi-active MSK which updates the gap-size, based on the control methodology described in the previous section, in quasi-real-time. The second model differs in that it has a fixed initial end joint gap. This study describes the two models as the model with a varying gap (VG) and the model with a constant gap (CG). Several NLRHAs are conducted to evaluate the performance of the semi-active controller and the effect of gap variation on the seismic performance of the bridge. The effectiveness of the proposed control

methodology to operate the MSKs is evaluated by comparing its responses against the model with the constant gap.

A set of seven design-spectrum compatible earthquake ground motion accelerograms is used for the NLRHA. These ground motions are the ones used in [8] and are scaled to different PGA levels of seismic intensity starting from 0.08g to 0.96g at an increment of 0.08 g. The lowest level of seismic action was considered as 50% of the design earthquake, which is at 0.08 g, and the highest at 0.96g which is six times the design earthquake (to be able to reach LS4)

3.2 Illustration of proposed control methodology

The adaptability of the proposed semi-active control strategy is demonstrated through its ability to engage or disengage the MSKs when seismic responses exceed predefined limits (see Section 2). This is illustrated in the time-history plot of the gap size, as shown in Figure 3. The analysis begins with an initial gap of 50 mm and around the 5s mark, the controller is activated, which leads to opening of the gap. The gap size is adjusted based on the current displacement of the deck so that the gap is closed to transfer the force to the abutment-backfill system or open to avoid transferring of the force to the abutment-backfill system. Following this, the gap dynamically varies in response to the signal from the controller, adjusting to the seismic demands. The analysis concludes with the gap returning to a closed position, highlighting the ability of the controller to manage the gap size effectively throughout the seismic event. This dynamic adjustment underscores the system's adaptability and responsiveness in enhancing the bridge's seismic performance.

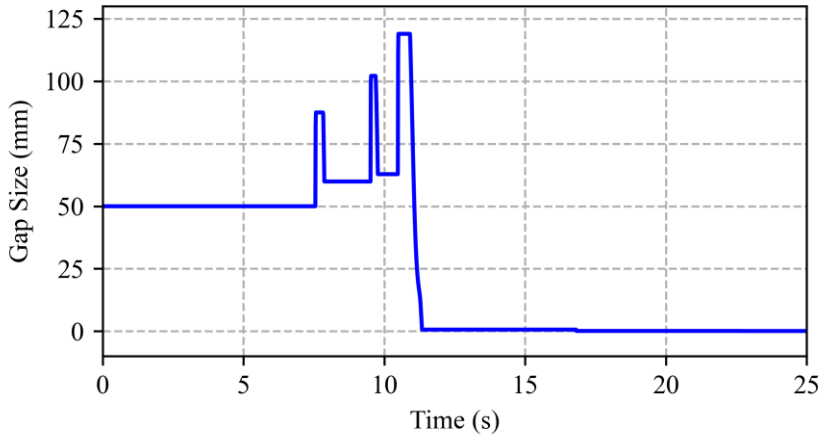

Figure 3 Time history of the longitudinal gap size.

The performance of the proposed semi-active controller is further evaluated by analysing the force-displacement response of the abutment-backfill system. Figure 4 illustrates the hysteresis loops for both models considered for the study: the constant gap model (CG) with a fixed initial gap of 50 mm and the variable gap model (VG). In both cases, the first loading branch initiates at 50 mm, corresponding to the closure of the initial gap. For the CG model, the initial gap remains constant throughout the analysis. The hysteresis loop for the CG model exhibits a regular, repeating pattern. However, in the VG model, multiple hysteresis loops appear, indicating the dynamic opening and closing of the gap throughout the analysis. Here, the negative displacement values account for the movement of the deck in the opposite direction (away from the abutment).

The effect of initial gap sizes on the PGA threshold for limit state exceedance for both bridge models (CG and VG) is shown in Figure 5. It is observed from the figure that for CG the

maximum PGA threshold for both limit states are obtained for an initial gap size of 50 mm. However, for the VG model, the initial gap size does not influence the PGA threshold values suggesting that the variable gap device can adapt to different seismic demands regardless of the initial gap size. This shows the robustness and adaptability of the proposed control system.

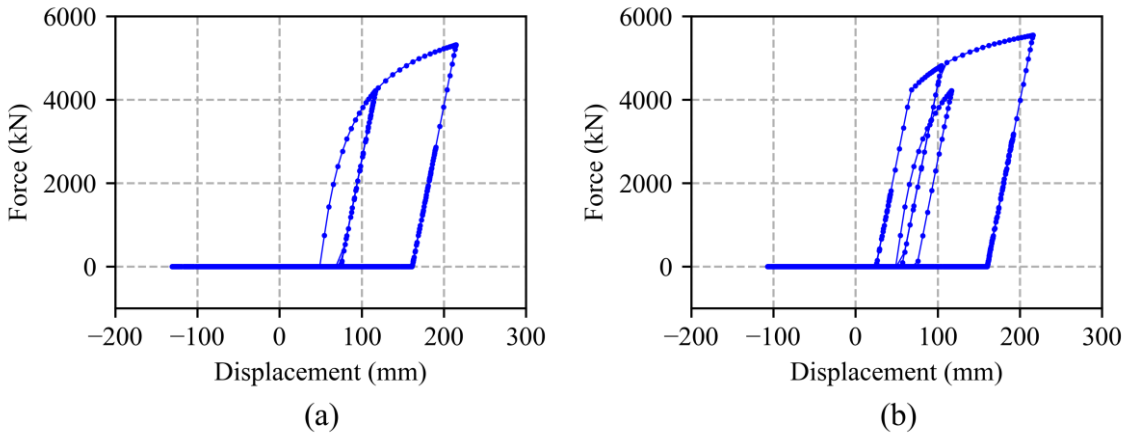

Figure 4 Force-displacement history for the abutment-backfill for the two bridge models: (a) CG, (b) (VG)

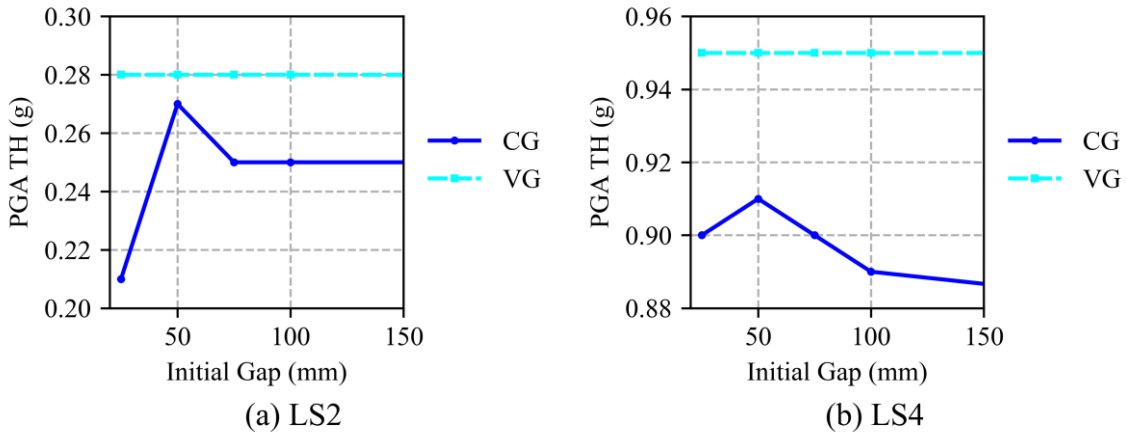

Figure 5 Variation of PGA thresholds with different initial gap sizes for (a) LS2 (b) LS4

3.3 Parametric investigation of Safety Factor Limits

As explained in the methodology, the $\lambda_{lim,i}$ values govern the activation of the semi-active MSKs and have a significant influence on the seismic responses. Hence, a parametric study is conducted to choose the best values of the limiting global safety factors ($\lambda_{lim,i}$) corresponding to each limit state. For the analysis, different ranges of values are selected for both limiting values corresponding to LS2 and LS4. For $\lambda_{lim,i}$ the range selected is from 1 to 3 with increments of 0.1, allowing for a detailed exploration of how varying limiting values of safety factors impact the structural response at this limit state. By systematically evaluating these ranges, the study aims to identify the most effective $\lambda_{lim,i}$ values that ensure optimal performance of the semi-active device across both limit states.

To find the values of $\lambda_{lim,i}$ that optimise the response of the bridge, the effect of variation of $\lambda_{lim,i}$ on the seismic responses of the bridge with the variable gap (VG) are studied. Based on the results of the NLRHA of the bridge the values of λ_i (A_g) for the seven ground motions for each intensity are calculated for each limit state and corresponding to these values, the PGA

threshold at which, each limit state is exceeded is calculated. The value of the $\lambda_{lim,i}$ at which the maximum PGA threshold (of the pertinent LS) is obtained is the optimum value. Figure 6 shows the variation of the average PGA threshold exceeding LS2 for different values of $\lambda_{lim,LS2}$. It is seen that the values vary between 0.262 g to 0.276 g, indicating that the values fall within a narrow range. As evident from the figure, the best value of $\lambda_{lim,LS2}$ =2.1 corresponds to the maximum value of the PGA threshold which is 0.276g. This value ensures that the bridge can endure the highest seismic intensity before reaching LS2, making it the optimal choice for this limit state. Similarly, Figure 6 shows the variation of the average PGA threshold corresponding to LS4 for different values of $\lambda_{lim,LS4}$. The maximum value of the PGA threshold is obtained as 0.946 g which corresponds to $\lambda_{lim,LS4}$ =1.6 which is the best option.

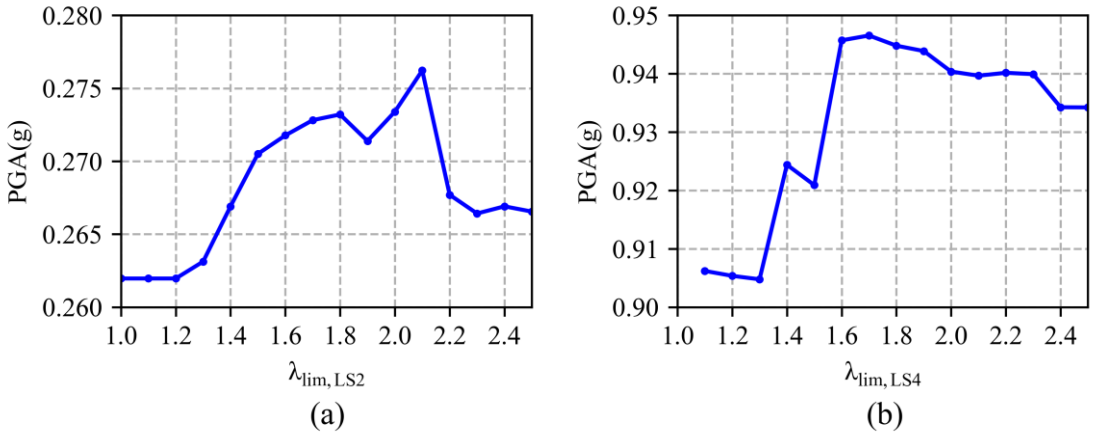

Figure 6 Variation of PGA threshold for λ_i exceedance for different values of $\lambda_{lim,i}$

To evaluate the performance of the proposed controller the effectiveness of the controller in maximizing the global safety factor (λ_i) is studied. The λ_i values of the bridge with the varying gap (VG) are compared with the model with a constant gap (CG). The controller focuses on maximizing the global safety factor values thereby improving the safety of the components. The percentage change λ_i (%) in the λ_i value is calculated as shown in equation 5.

$$\lambda_i(\%) = \frac{\lambda_i(VG) - \lambda_i(CG)}{\lambda_i(CG)} \times 100, \tag{3}$$

where λ_i (VG) is the global safety factor of the bridge model with the controller which updates the gap throughout the analysis and hence has a varying gap size, λ_i (CG) is the global safety factor of the bridge model with no controller and has a constant gap value which is initialized at the start of the analysis. The percentage improvement in the λ_i is plotted against the limiting values of $\lambda_{lim,i}$ in Figure 7 for each limit state. The percentage change in λ_2 increases for higher values of $\lambda_{lim,LS2}$ (Figure 7 (a)) and for different ground motion intensities it is in the range of 4% to 25% for all values of $\lambda_{lim,LS2}$ >1.7. At lower intensities (0.16 g to 0.32 g), the improvement is around 3% to 5%, whereas for higher intensities (0.40 g to 0.56 g), it increases to 10%–25%. This trend can be explained by the exceedance of LS2 occurring at a PGA of 0.276 g. At lower earthquake intensities, the components reach the LS threshold less frequently compared to cases where the PGA threshold is exceeded. Similarly, the percentage improvement in λ_4 is in the range of 4-9 % as shown in Figure 7 (b). The exceedance of LS4 occurs at a PGA of 0.94 g and the percentage improvement is noticed to be higher in case of the higher earthquake intensities (0.88 g-1.04g) close to this value than the lower intensities.

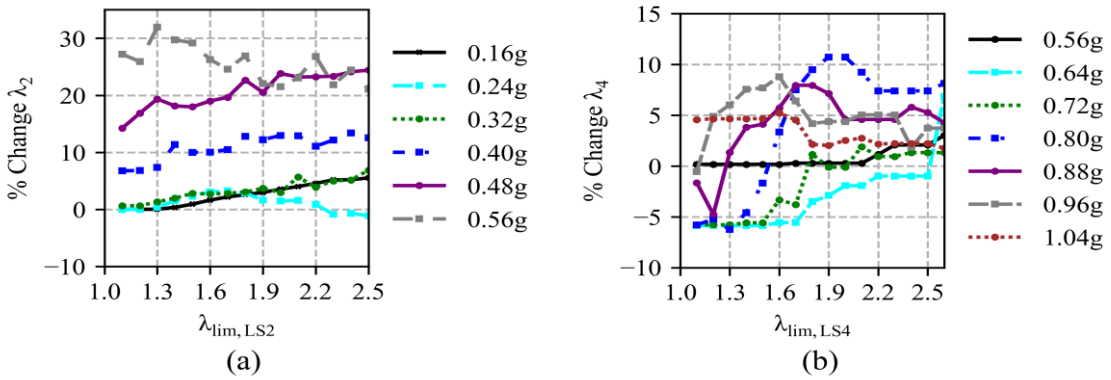

Figure 7 Percentage change in global safety factor with the variation of (a) $\lambda_{lim,LS2}$, (b) $\lambda_{lim,LS4}$

4 CONCLUSIONS

The present study puts forward a semi-active MSK which operates based on real-time displacement thresholds, opening and closing a joint when the seismic response exceeds predefined limits based on the safety factor against exceeding specific LS. This adaptability is achieved through a closed-loop feedback control strategy, which continuously adjusts the position of the shear key in real time. The control algorithm is designed to regulate bridge gaps by dynamically positioning the adjacent MSKs, enhancing the protection of critical bridge components. The performance of the control strategy is evaluated through response history analyses conducted on a bridge model with and without MSKs.

Numerical results demonstrate that semi-active MSKs can reduce the peak responses and enhance overall seismic performance. The results of the NLRHAs demonstrate that the proposed semi-active controller effectively maximizes the global safety factor by increasing the PGA thresholds for the bridge with MSKs compared to the one without.

To refine the control strategy, a parametric analysis was conducted on the effect of the safety factor limit, $\lambda_{lim,i}$ which governs the activation of the semi-active device. The parametric study identified the optimal values of $\lambda_{lim,LS2}$ as 2.1 and $\lambda_{lim,LS4}$ as 1.6, which corresponds to the maximum PGA thresholds for their respective limit states. These values ensure that the bridge, equipped with the semi-active MSK device, achieves the highest possible seismic resilience while maintaining safety and performance across both limit states. The results highlight the importance of carefully selecting $\lambda_{lim,i}$ values to optimize the seismic response of structures under varying levels of seismic intensity. However, these findings are strictly valid only for the bridge type studied. Therefore, further parametric studies should be performed for different bridge configurations to fine-tune the global safety factor thresholds effectively.

Furthermore, the results demonstrate the effectiveness of the controller under varying seismic conditions and initial gap sizes. The analysis shows that while the performance of the bridge model with the constant gap (CG) is dependent on the initial gap size, the performance of the proposed semi-active model (VG) remains consistent across different initial gap sizes due to the adaptability of the variable gap device. This adaptability highlights the robustness and effectiveness of the proposed control system in the VG model, making it a potentially superior choice for enhancing the seismic performance of bridges.

ACKNOWLEDGEMENT

The authors gratefully acknowledge the financial support by Khalifa University, Abu Dhabi [research project reference number: RIG-2023-006, Principal Investigator: A. Kappos].

REFERENCES

[1] K. Kawashima and S. Unjoh, "The damage of highway bridges in the 1995 Hyogo-ken Nanbu earthquake and its impact on Japanese seismic design," *Journal of Earthquake Engineering*, vol. 1, no. 3, pp. 505–541, 1997, doi: 10.1080/13632469708962376.

[2] A. Pamuk, E. Kalkan, and H. I. Ling, "Structural and geotechnical impacts of surface rupture on highway structures during recent earthquakes in Turkey," *Soil Dynamics and Earthquake Engineering*, vol. 25, no. 7–10, pp. 581–589, Aug. 2005, doi: 10.1016/j.soildyn.2004.11.011.

[3] T. Banerjee, D. Ghosh, and D. Das, "A state-of-the-art review and future challenges on application of devices for vibration control of bridges," *Mechanics of Advanced Materials and Structures*, pp. 1–27, Feb. 2025, doi: 10.1080/15376494.2025.2462713.

[4] K. I. Gkatzogias and A. J. Kappos, "Semi-active control systems in bridge engineering: A review of the current state of practice," 2016, *Int. Assoc. for Bridge and Structural Eng. Eth-Honggerberg*. doi: 10.2749/101686616X14555429844040.

[5] CEN (2005b), *Eurocode 8: Design of Structures for Earthquake Resistance–Part 2: Bridges.* Brussels, Belgium: European Committee for Standardization, Brussels, 2005.

[6] Caltrans, "Seismic Design Criteria Version 2.0," CA, USA, 2019.

[7] A. J. Kappos, "The dynamic intelligent bridge: A new concept in bridge dynamics," in *Geotechnical, Geological and Earthquake Engineering*, vol. 47, Springer Netherlands, 2019, pp. 373–383. doi: 10.1007/978-3-319-78187-7_28.

[8] I. G. Mikes and A. J. Kappos, "Optimization of the seismic response of bridges using variable-width joints," *Earthquake Engineering and Structural Dynamics*, vol. 52, no. 1, pp. 111–127, 2023, doi: 10.1002/eqe.3751.

[9] I. G. Mikes, A. J. Kappos, and A. Giaralis, "Effect of abutment-backfill limit state definition on the assessment of seismic performance," in *3rd International Conference on Natural Hazards & Infrastructure*, Jul. 2022. [Online]. Available: http://openaccess.city.ac.uk/publications@city.ac.uk

[10] G. Mylonakis, S. Nikolaou, and G. Gazetas, "Footings under seismic loading: Analysis and design issues with emphasis on bridge foundations," *Soil Dynamics and Earthquake Engineering*, vol. 26, no. 9, pp. 824–853, Sep. 2006, doi: 10.1016/j.soildyn.2005.12.005.

[11] F. Naeim and J. M. Kelly, "Design of Seismic Isolated Structures: From Theory to Practice. .," *John Wiley & Sons,Inc.*, vol. New York, no. USA, 1999.

[12] P. Khalili-Tehrani, A. Shamsabadi, J. P. Stewart, and E. Taciroglu, "Backbone curves with physical parameters for passive lateral response of homogeneous abutment backfills," *Bulletin of Earthquake Engineering*, vol. 14, no. 11, pp. 3003–3023, Nov. 2016, doi: 10.1007/s10518-016-9934-3.

[13] I. G. Mikes and A. J. Kappos, "Modelling of the post-peak response of abutment-backfill systems: a new hysteretic model for OpenSees," *Bulletin of Earthquake Engineering*, vol. 22, no. 5, pp. 2723–2737, Mar. 2024, doi: 10.1007/s10518-024-01870-8.

[14] A. Bozorgzadeh, S. A. Ashford, and J. I. Restrepo, "Effect of backfill soil type on stiffness and ultimate capacity of bridge," in *Geotechnical Earthquake Engineering and Soil Dynamics IV*, San Diego: University of California.: ASCE, 2008.

[15] I. G. Mikes and A. J. Kappos, "Simple and complex modelling of seat-type abutment-backfill systems," in *COMPDYN Proceedings*, M. Papadrakakis and M. Fragiadakis, Eds., Athens, Greece, Jun. 2021, pp. 5266–5282. doi: 10.7712/120121.8864.19520.